Texture of Cu(In,Ga)Se_2 thin films and nanoscale cathodoluminescence

2004 J. Phys.: Condens. Matter 16 S85

(http://iopscience.iop.org/0953-8984/16/2/010)

INSTITUTE OF PHYSICS PUBLISHING JOURNAL OF PHYSICS: CONDENSED MATTER

J. Phys.: Condens. Matter **16** (2004) S85–S89 PII: S0953-8984(04)66907-4

Texture of $Cu(In, Ga)Se_2$ thin films and nanoscale cathodoluminescence

N Ott[1], G Hanna[2], U Rau[2], J H Werner[2] and H P Strunk[1]

[1] Universität Erlangen-Nürnberg, Institut für Werkstoffwissenschaften, Lehrstuhl für Mikrocharakterisierung, Cauerstraße 6, 91058 Erlangen, Germany
[2] Universität Stuttgart, Institut für Physikalische Elektronik, Pfaffenwaldring 47, 70569 Stuttgart, Germany

Received 31 July 2003
Published 22 December 2003
Online at stacks.iop.org/JPhysCM/16/S85 (DOI: 10.1088/0953-8984/16/2/010)

Abstract

We investigate the microstructure of $Cu(In, Ga)Se_2$ thin films with different preferred grain orientations (textures). The films are grown by coevaporation from elemental sources. We analyse the electro-optical properties of the films with a cathodoluminescence spectrometer attached to a transmission electron microscope. {112} textured films show sharp contrasts at the grain boundaries, whereas grain boundaries in {220/204} textured films give only very weak contrasts indicating a preferential population of electronically rather inactive grain boundaries.

1. Introduction

One of the promising families of materials for solar cell use is the thin film chalcopyrites $Cu(In, Ga)Se_2$ (CIGS). Since Contreras *et al* [1] showed that their absorber layers leading to the record efficiency of 18.8% had a {220/204} texture (preferred grain orientation) in contrast to the {112} texture or random orientation of previous high efficiency cells (up to 17.7% efficiency), the influence of the texture on the cell performance has been a matter of interest. We analyse in this paper the optoelectronic properties of CIGS absorber layers with different textures by analysing their cathodoluminescence (CL) properties. As the CIGS films are polycrystalline with average grain sizes of around 1 μm a high spatial resolution is necessary for the investigations. In view of this we use for our studies a transmission electron microscope (TEM) with an attached CL spectrometer.

2. Experimental details

The CIGS films were grown by coevaporation from elemental sources. All CIGS films treated here are Cu poor and have a Ga/(In + Ga) ratio of 0.28. We grew different samples by the three-stage process [2]. Two samples were grown directly on Mo-coated glass substrates, but with different Se rates at different temperatures. We call these samples high T and low T.

One sample was grown with a sodium diffusion barrier (aluminium oxide) between the Mo layer and the glass (i.e. with no diffusion of sodium into CIGS from the glass). In this case the sodium source for the layer consisted of a NaF layer between the Mo layer and the CIGS film grown. We thus call this sample the NaF precursor sample. The texture of the films was determined by means of x-ray diffraction (XRD).

The TEM investigations require specially treated samples. These TEM specimens were prepared by cutting small pieces from the film which were then mechanically ground from the back. After all of the glass was removed we glued a Ni ring on the TEM specimen for stabilization. Ar ion milling under liquid nitrogen cooling finally leads to electron transparency.

The TEM specimens were then analysed in a Philips CM30 TEM, to which a Gatan MonoCL2 CL system is attached with a liquid nitrogen cooled Ge detector. The CL analysis (local spectra and CL mappings) were made at an accelerating voltage of 150 kV while the specimen was cooled with liquid nitrogen to approximately $-180\,^{\circ}\mathrm{C}$. The structures of these areas were then analysed by a scanning transmission electron microscope (STEM) imaging in the bright-field (BF) mode.

3. Results

3.1. Texture of the films

All our samples have either {112} or {220/204} texture of the sample normal. The {220/204} texture is ambiguous since the orientations {220} and {204} cannot be distinguished because of overlapping XRD peaks (the CIGS has a tetragonal chalcopyrite structure with an c/a ratio close to 2). The high T sample shows a {220/204} texture in contrast to the {112} texture of the low T and the NaF precursor samples. Hanna *et al* [3] give more details on growing textured CIGS films.

3.2. CL mappings

Figures 1(a)–(f) show panchromatic CL mappings of the different samples and corresponding BF STEM images. The low T sample (figure 1(a)) shows a prominent structure in the CL mapping consisting in bright areas separated by dark lines. These sharp dark lines indicate less CL intensity and thus enhanced non-radiative recombination. Comparison with the TEM image of the same area (figure 1(b)) shows that the dark lines coincide with grain boundaries.

The CL mapping of the NaF precursor sample (figure 1(c)) also shows bright areas separated by dark lines. In comparison with those for the low T sample (figures 1(a), (b)), the bright areas are smaller. Again by comparing the CL mapping and the TEM image (figure 1(d)) we see that the dark lines correspond to grain boundaries. In addition the grains contain more structural defects than those in the low T sample.

The high T sample shows almost no contrast in the CL mapping (figure 1(e)). The contrast settings for this image were much higher than for the previous images. The image shows an almost constant CL intensity over the whole imaged area. In particular, when we compare the mapping with the TEM image of the same area (figure 1(f)), we see no correlation of the grain boundaries with features in the CL mapping. The small differences in the luminescence intensity are very probably due to thickness variations of the specimen.

3.3. CL spectra

Figures 2(a)–(c) show CL spectra of the samples. All samples show only one broad peak, but the peak position varies somewhat. While both {112} textured samples show a peak at

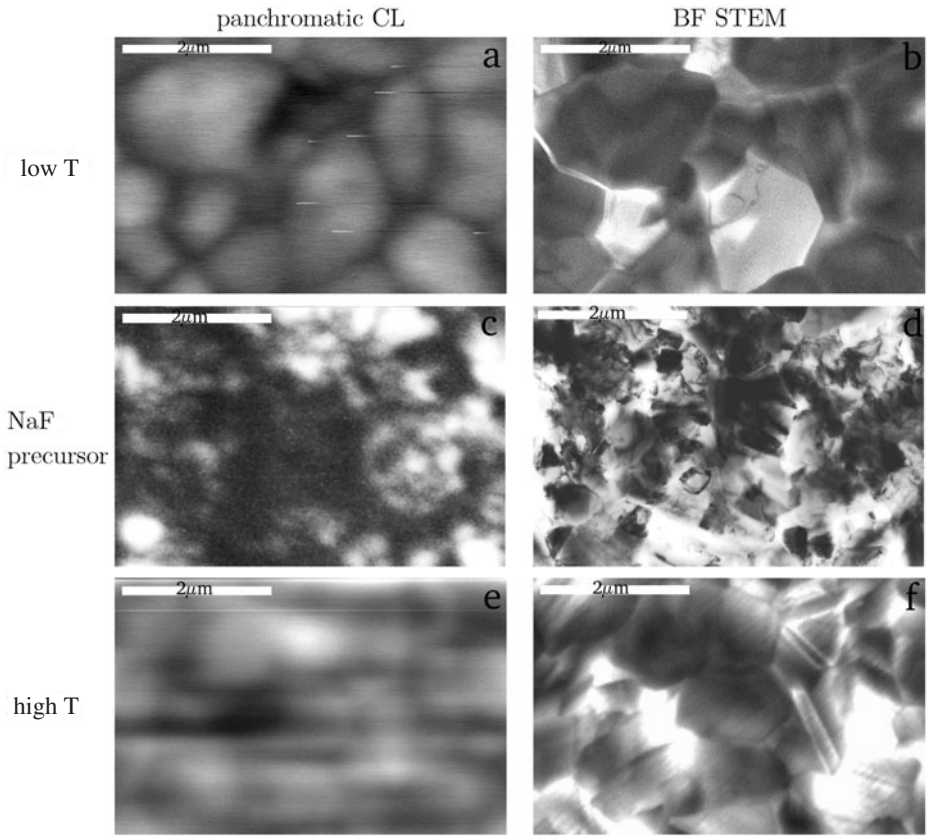

Figure 1. Panchromatic CL mappings and the corresponding BF STEM images of the same area. (a) A CL mapping of the low T sample showing sharp contrasts at grain boundaries, (b) a STEM image of the low T sample showing only few defects inside the grains, (c) a CL mapping of the NaF precursor sample showing sharp contrasts at grain boundaries and defects, (d) a TEM image of the NaF precursor sample showing many defects inside the grains, (e) a CL mapping of the high T sample showing almost no contrast, (f) a STEM image of the high T sample showing only few defects inside the grains.

0.97 eV, the {220/204} textured sample shows a peak at 1.08 eV. The absolute intensity of the emission cannot be compared between the three samples, because the thicknesses of the specimens and the distances between sample and mirror (for the detection system, i.e. the collection efficiency) can be different. The spectra show no difference whether they are taken from an area with a diameter of 50 or of 0.5 μm (single grain).

4. Discussion

Table 1 summarizes the CL results. Obviously there is a correlation with the texture type, which will be considered in the following.

4.1. CL mappings

The {220/204} textured film shows an almost homogeneous CL intensity, with no correlation of the still detectable fluctuations with the structural features, whereas the {112} textured films show lower intensity, in the form of dark lines, at structural defects, especially at the

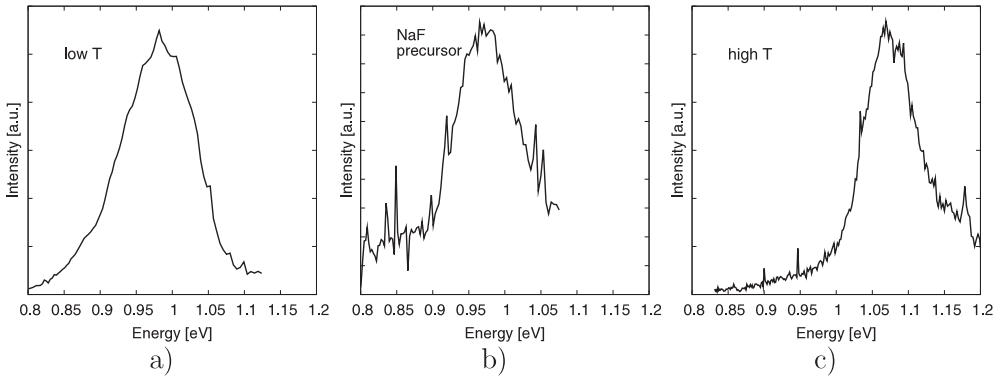

Figure 2. CL Spectra (area $\approx$ 3500 μm^2) of our different samples, all showing a single broad peak. (a) A low T sample, with a peak at 0.97 eV; (b) a NaF precursor sample, with a peak at 0.97 eV; and (c) a high T sample, with a peak at 1.08 eV.

Table 1. Overview of the different observed features for all samples.

Sample	Texture	CL peak position (eV)	CL contrasts
High T	{220/204}	1.08	Almost none
Low T	{112}	0.97	At defects
NaF precursor	{112}	0.97	At defects

grain boundaries. In consequence the {112} textured films contain grain boundaries that represent strong non-radiative recombination paths. This behaviour is seen in both {112} samples independent of whether the films are of low T rate or NaF precursor type. Obviously the {220/204} texture results in beneficial grain boundary types with only a weak electrical activity. It is thus preferable for the solar absorber layers, as is in fact indicated by the work of Contreras *et al* [1].

4.2. CL spectra

The variation in the peak positions of the CL spectra between {112} and {220/204} texture cannot be explained by the different grain boundary types. Spectra obtained from interiors of individual grains show the same features as spectra taken from large parts of the sample. The single broad peak arises supposedly from transitions due to fluctuating potentials. There is independent evidence due to several groups who showed that photoluminescence spectra from Cu-poor CIGS films, either polycrystalline [4] or monocrystalline [5], are characterized by fluctuating potentials. Thus the shift of the peak between {112} and {220/204} textures might be due to shifts of the (average) band gap.

5. Summary

We have presented CL studies of CIGS thin films, with different preferred grain orientations of the films: either {220/204} or {112} texture. CL mappings showed that the {112} textured samples contain a grain boundary population that reduces the CL; i.e. grain boundaries provide non-radiative recombination paths. The {220/204} texture, however, causes a rather inactive

grain boundary population which may be the reason for the record efficiency solar cell made from material of this type [1].

Acknowledgments

Part of this work was carried out in the Central Facility for High Resolution Electron Microscopy of Friedrich-Alexander University Erlangen-Nürnberg, Germany. The German Federal Ministry of Education and Research (BMBF) under contract No 01SF0113 (Hochspannungsnetz) supported this work.

References

[1] Contreras M A, Egaas B, Ramanathan K, Hiltner J, Swartzlander A, Hasoon F and Noufi R 1999 *Prog. Photovolt. Res. Appl.* **7** 311
[2] Gabor A M, Tuttle J R, Albin D S, Contreras M A, Noufi R and Hermann A M 1994 *Appl. Phys. Lett.* **65** 198
[3] Hanna G, Mattheis J, Laptev V, Yamamoto Y, Rau U and Schock H W 2003 *Thin Solid Films* **431/432** 31
[4] Dirnstorfer I, Wagner M T, Hofmann D M, Lampert M D, Karg F and Meyer B K 1998 *Phys. Status Solidi* a **168** 163
[5] Rega N, Siebentritt S, Beckers I E, Beckmann J, Albert J and Lux-Steiner M Ch 2003 *Thin Solid Films* **431/432** 186